Journal of Integrative Neuroscience

J. Integr. Neurosci. **2024**; 23(8): 142
https://doi.org/10.31083/j.jin2308142

Original Research

Fingolimod Alleviates Inflammation after Cerebral Ischemia via HMGB1/TLR4/NF-κB Signaling Pathway

Yao Xing[1,†], Liyuan Zhong[2,3,†], Jun Guo[1], Cuifen Bao[1], Yumin Luo[2,3,*], Lianqiu Min[1,*]

[1]Department of Neurology, The First Affiliated Hospital of Jinzhou Medical University, 121001 Jinzhou, Liaoning, China
[2]Institute of Cerebrovascular Disease Research, Xuanwu Hospital of Capital Medical University, 100053 Beijing, China
[3]Department of Neurology, Xuanwu Hospital of Capital Medical University, 100053 Beijing, China
*Correspondence: yumin111@ccmu.edu.cn (Yumin Luo); MinLQ@jzmu.edu.cn (Lianqiu Min)
[†]These authors contributed equally.
Academic Editor: Gernot Riedel
Submitted: 29 March 2024 Revised: 18 May 2024 Accepted: 27 May 2024 Published: 12 August 2024

Abstract

Background: Clinically, ischemic reperfusion injury is the main cause of stroke injury. This study aimed to assess the effectiveness of fingolimod in suppressing inflammation caused by ischemic brain injury and explore its pharmacological mechanisms. **Methods**: In total, 75 male Sprague-Dawley rats were randomly and equally assigned to five distinct groups: sham, middle cerebral artery occlusion/reperfusion (MCAO/R) surgery, fingolimod low-dose (F-L), fingolimod medium-dose (F-M), and fingolimod high-dose (F-H). Neurobehavioral tests, 2,3,5-triphenyltetrazolium chloride staining, and the brain tissue drying-wet method were conducted to evaluate neurological impairment, cerebral infarction size, and brain water content. Enzyme-linked immunosorbent assay was employed to quantify pro-inflammatory cytokines interleukin (IL)-1β, IL-6, and tumor necrosis factor-alpha (TNF-α) protein levels. Western blotting and immunohistochemical staining were performed to assess high mobility group box 1 (HMGB1), toll-like receptor 4 (TLR4), and nuclear factor kappa-B p65 (NF-κBp65) levels. **Results**: Rats in the F-L, F-M, and F-H groups exhibited lower Longa scores, reduced infarction volumes, and decreased brain edema than those in the MCAO/R group. Additionally, the F-L, F-M, and F-H groups exhibited lower serum levels of IL-1β, IL-6, and TNF-α than those of the MCAO/R group. Additionally, F-L, F-M, and F-H treatments resulted in decreased HMGB1, TLR4, and NF-κBp65 protein expression levels in the hippocampus of MCAO/R rats. **Conclusions**: Fingolimod was found to reduce ischemic brain injury in a dose-dependent manner. Moreover, it was also found to alleviate inflammation following ischemic brain injury via the HMGB1/TLR4/NF-κB signaling pathway.

Keywords: fingolimod; inflammation; ischemic injury; HMGB1; TLR4; NF-κB

1. Introduction

As the most prevalent type of cerebrovascular disease, ischemic stroke imposes an apparent financial burden on affected patients, their families, and even the entire society [1]. It occurs owing to narrowing or complete blockage of the cerebral blood vessels, resulting in irreversible neuronal cell death and neurological impairment [2,3].

Cerebral ischemic injury triggers a strong inflammatory response, which is a critical characteristic of ischemic stroke pathology that occurs within hours of blood vessel blockage. This inflammatory response significantly increases the levels of inflammatory cytokines, including interleukin (IL)-6 and tumor necrosis factor-alpha (TNF-α), thereby exacerbating cerebral ischemic injury [4]. Hence, suppressing excessive inflammation potentially represent a hopeful treatment strategy aimed at reducing the severity of ischemic brain damage.

Immediate restoration of cerebral blood flow to salvage the infarcted cerebral hemisphere is the most efficient therapeutic approach for ischemic stroke. Currently, intravenous thrombolysis using a recombinant tissue plasminogen activator is a relatively safe and widely accepted treatment for ischemic stroke. However, this method can result in cerebral ischemia/reperfusion injury, as well as a cascade of intricate processes, which encompass inflammation, oxidative stress, apoptosis, and autophagy [5]. Therefore, it is crucial to explore and develop novel and reliable strategies and medications that not only restore cerebral blood flow but also alleviate ischemic brain injury.

Fingolimod, also known as FTY720, is synthesized through the chemical modification of myriocin, an extract of *Cordyceps sinensis* [6]. Additionally, fingolimod, an immunosuppressive medication that has been given the green light by the Food and Drug Administration (FDA) for its use in treating multiple sclerosis, is essential for maintaining vascular integrity, lymphocyte transport, and immune response modulation [6,7]. A clinical study found that patients with acute ischemic stroke who received short-term fingolimod therapy alongside standard stroke therapy exhibited a decrease in microvascular permeability, secondary injury, and better clinical outcomes [8]. However, the underlying pharmacological mechanisms of action of fingolimod in ischemic brain injury remain to be fully understood.

This study aimed to investigate the effects and mechanisms of action of various doses of fingolimod on ischemic brain injury. First, we assessed the neuroprotective efficacy of various doses of fingolimod in ischemic brain injury. Subsequently, we explored the physiological role of various doses of fingolimod in protecting against inflammation after experiencing cerebral ischemia. Additionally, we investigated the underlying pharmacological mechanisms of fingolimod in inflammation induced by ischemic brain injury, utilizing a rat model that simulates transient focal cerebral ischemia.

2. Materials and Methods

2.1 Experimental Animals

The animal experiments adhered to the protocols outlined in the National Institutes of Health's "Guide for the Care and Use of Laboratory Animals" and received approval from the Animal Care and Use Committee at Jinzhou Medical University (2022022701). A total of 75 clean, healthy male Sprague Dawley (SD) rats weighing between 250 and 280 grams and aged 8 to 9 weeks, were supplied by the Experimental Animal Center at Jinzhou Medical University (Jinzhou, China). On day 3 after adaptive feeding, rats were randomly allocated into different groups (n = 15): (1) sham group, (2) middle cerebral artery occlusion/reperfusion (MCAO/R) surgery group, (3) fingolimod low-dose (F-L) group (0.5 mg/kg), (4) fingolimod medium-dose (F-M) group (1.0 mg/kg), (5) fingolimod high-dose (F-H) group (2.0 mg/kg).

2.2 Drug Administration

Fingolimod (Cat #HY-11063, MedChemExpress, Monmouth Junction, NJ, USA) was prepared in dimethylsulfoxide (DMSO, D8371, Beijing Solebao Technology Co., Ltd., Beijing, China) and diluted in a 0.9% NaCl saline solution to final concentrations (0.5, 1.0, and 2.0 mg/kg). On days 0 (immediately after MCAO) and 1 (24 h) after MCAO, rats in the MCAO/R group were intraperitoneally administered normal saline containing DMSO, whereas rats in the F-L, F-M, and F-H groups were intraperitoneally administered the same volume of fingolimod at different concentrations (0.5, 1.0, and 2.0 mg/kg).

2.3 Transient Rat Middle Cerebral Artery Occlusion (MCAO) Model

MCAO procedure was executed using an adapted thread embolism method, as outlined in prior research [9]. The rats were anesthetized by placing them in a chamber containing a mixture of 4.0–5.0% isoflurane (Cat# R510, RWD Life Science, Shenzhen, Guangdong, China) and oxygen and then maintained during MCAO surgery with 1.5–2.0% isoflurane in a mixture of 70% N_2O and 30% O_2. Once anesthesia was stable, the rats were positioned on the surgical operating table with their limbs secured. Before surgery, the fur around the neck was shaved with a blade and disinfected using povidone-iodine and 70% ethanol.

A median incision approximately 4 cm in length was made in the middle of the neck. The subcutaneous fat and surrounding connective tissue were carefully stripped to expose the carotid sheath and dissected to expose the common carotid artery (CCA), internal carotid artery (ICA), and external carotid artery (ECA). The superior thyroid and the occipital arteries were isolated and electrocoagulated. The CCA and ICA were temporarily clamped, and the ECA was ligated with a nylon monofilament at the distal end. A V-shaped incision was made at the distal end of the ECA at a 45° angle. Subsequently, a monofilament nylon suture (Beijing Xinong Biotechnology Co., Ltd., Beijing, China) was gently inserted into the ICA via the incision until mild resistance was felt (approximately 18–20 mm distal to the carotid bifurcation).

The filament was removed 2 h after MCAO to restore cerebral blood flow. Hemostasis was checked, and the wound was closed using nylon sutures. For rats in the sham group, the CCA was isolated without ligation or hypoxia. The rats' rectal temperature was maintained at approximately 37.0 $\pm$ 0.5 °C throughout the MCAO surgical process. After surgery, all rats were allowed to move freely, eat, and drink in their cages.

2.4 Neurological Deficit Score

The Zea-Longa score was used to evaluate neurological recovery following the method described in a previous study [10]. The scoring system ranges from 0 to 4, with the following interpretations: 0 = no apparent neurological deficits, 1 = incomplete extension of the left forelimb, 2 = a leftward circling motion, 3 = left-sided weakness, and 4 = the absence of spontaneous walking and a lack of consciousness.

2.5 2,3,5-Triphenyltetrazolium Chloride (TTC) Staining

The rats were humanely sacrificed 2 h after the second administration of the drug by administering excessive anesthesia (amobarbital; Cat #17784, Cayman Chemical Company, Ann Arbor, MA, USA, 10%, 0.5 mL/100 g). After cardiac perfusion, rat brains were excised through decapitation and then cut into 2 mm thick coronal sections. These slices were then placed in a 2% 2,3,5-Triphenyltetrazolium Chloride (TTC, T8877, Sigma, Burlington, MA, USA) solution and incubated at 37 °C for 10 min. Subsequently, slices were fixed with 4% paraformaldehyde. The infarct volume was assessed using ImageJ software (version 1.5, NIH, Bethesda, MD, USA). To calculate the percentage of the ischemic lesion area, we used the following equation: infarct volume (%) = (volume of contralateral hemisphere – volume of non-infarcted ipsilateral hemisphere)/volume of contralateral hemisphere $\times$ 100%.

2.6 Brain Water Content

The rats were euthanized 2 h after the second administration of the drug under excessive anesthesia (amobarbital; Cat# 17784, Cayman Chemical Company, Ann Arbor, MA, USA, 10%, 0.5 mL/100 g). Subsequently, cerebral tissue was derived from rats without myocardial perfusion. The humidity of the cerebral tissue was assessed immediately after the rats were sacrificed. The cerebral tissue was microwave-dried in a microwave oven at 100 °C until the cerebral weight remained constant, known as dry weight. Brain water content was assessed using the following formula: brain water content (%) = [(humid brain weight – dry brain weight)/humid brain weight] $\times$ 100.

2.7 Enzyme-Linked Immunosorbent Assay (ELISA)

Pro-inflammatory factors TNF-α (Cat# ml003057), IL-1β (Cat# ml064292), and IL-6 (Cat# ml002859) levels were assessed via commercially available kits purchased from Shanghai Enzyme-linked Biotechnology Limited Company (Shanghai, China). The rats were euthanized 2 h after administration of the second drug under excessive anesthesia (amobarbital; Cat# 17784, Cayman Chemical Company, Ann Arbor, MA, USA, 10%, 0.5 mL/100 g). Blood samples were collected from the heart via needle aspiration and transferred to Rapid Serum Tubes for serum sample collection. The samples were then centrifuged at a speed of 3000 rpm for 10 min. Following this, the serum samples were carefully transferred into new cryovials for preservation at –80 °C for subsequent enzyme-linked immunosorbent assays (ELISA). Prior to the ELISA, the samples were thawed at room temperature. We performed ELISA according to the manufacturer's protocol using an ELISA kit (Shanghai Enzyme-linked Biotechnology Limited Company, Shanghai, China). The steps involved in the ELISA procedure were as follows: (1) Adding standard: 50 µL standards with different concentration gradients were added in different holes. (2) Adding samples: 40 µL of sample dilution was added to the holes, then 10 µL of the sample fluid was added. The contents were then mixed gently. (3) Adding enzyme: 100 µL of horseradish peroxidase (HRP)-conjugate reagent was added to the hole designated for the standard solutions and samples, excluding the blank hole. (4) Incubation: The plates secured with a seal and then placed in an incubator set to a temperature of 37 °C for a period of 60 min. (5) Washing: The sealing membrane was carefully taken off, and the liquid was subsequently was discarded. Washing liquid was poured into each hole, left for 30 s, and then poured out, and this step was repeated a total of five times. The 96-well plate was carefully patted and dried. (6) Color development: 50 µL of color developer A was carefully dispensed into each hole, after which an equal volume of color developer B, also 50 µL, was added. The mixture in each hole was then gently stirred to ensure thorough blending. Subsequently, the 96-well plate was placed in an incubator set to 37 °C and incubated for a duration of 15 min in a dark environment. (7) Stopping reaction: 50 µL of stop solution was poured into the hole, which halted the reaction and caused the color of each hole to change from blue to yellow. (8) Assay: The optical density (OD) for each well was determined using a microplate reader (Thermo Fisher Scientific, Waltham, MA, USA), with the readings taken at a wavelength of 450 nm. The blank well was set to zero, and readings were taken within 15 min of adding the stop solution.

2.8 Immunohistochemical Staining

Immunohistochemical staining was carefully conducted throughout the entire process according to a previously mentioned protocol [11]. Rat cerebral tissues were completely immersed in formalin, fixed, dehydrated, and embedded in paraffin wax. The paraffin-embedded cerebral tissue blocks mentioned above were then cut into 5 µm thick slices. The tissue slices were placed in fixation boxes containing citrate antigen retrieval buffer and fixed in a microwave oven. Once the slices had reached room temperature, they were immersed in a solution containing 3% hydrogen peroxide to block the activity of endogenous peroxidase and then immersed in phosphate-buffered saline (PBS) wash buffer three times. The slices were then incubated at 4 °C in the refrigerator with various primary antibodies: rabbit anti-high mobility group box 1 (HMGB1) antibody (1:500; Cat# ET1601-2, HuaAn Biotechnology, Hangzhou, Zhengjiang, China), rabbit toll-like receptor 4 (TLR4) antibody (1:400; Cat# ab22048, Abcam, Cambridge, MA, USA), and rabbit anti-nuclear factor kappa-B p65 (NF-κBp65) antibody (1:400; Cat# ab86299, Abcam, Cambridge, MA, USA). The next day, the slices were immersed in PBS wash buffer thrice for 5 min each. The sections were subsequently treated with horseradish peroxidase-labeled goat anti-rabbit/mouse secondary antibody for a duration of 20 min. After another three 5-minute washes with PBS wash buffer, the slices were subjected to color development using diaminobenzidine chromogenic solution. The sections were carefully washed with tap water, counterstained with hematoxylin, dehydrated, and made transparent. Finally, the slides were covered with neutral balsam and examined under a microscope. ImageJ software (version 1.5, NIH, Bethesda, MD, USA) was used to count the positive cells.

2.9 Western Blot Analysis

The infarcted rat hippocampus was lysed in radioimmunoprecipitation assay (RIPA) buffer (Cat #P0013B, Beyotime, Shanghai, China) containing a mixture of protease and phosphatase inhibitors. The mixture containing the lysate and tissue was subjected to centrifugation at a speed of 12,000 rpm for a duration of 30 min, and the supernatant was carefully poured into a new tube. The supernatant was gently mixed with sodium dodecyl sulfate-polyacrylamide gel electrophoresis (SDS-PAGE) loading buffer and then

heated at 95 °C for 5 min in a water bath. About 20 µg of protein was segregated and subsequently moved onto a polyvinylidene fluoride (PVDF) membrane (Millipore, Bedford, MA, USA) with a pore size of either 0.22 micrometers or 0.45 micrometers. To block nonspecific protein binding, the PVDF membrane was soaked in a solution containing 5% skim milk. After blocking, the membrane was then immersed in the following primary antibodies overnight at a controlled temperature of 4 °C within a refrigerated environment: anti-HMGB1 (1:1000; Cat# ET1601-2, HuaAn Biotecchnology, Hangzhou, Zhengjiang, China), anti-TLR4 (1:500, Cat# WL00196, WanLei Biotechnology, Shenyang, Liaoning, China), anti-NF-κBp65 (1:500, Cat# WL02169, WanLei Biotechnology, Shenyang, Liaoning, China), and anti-β-actin (1:10,000; Cat# AMC0001, ABclonal Technology, Wuhan, Hubei, China). After incubation with the primary antibodies, the membranes were then treated with secondary antibodies that had been conjugated with horseradish peroxidase (HRP): goat anti-rabbit IgG (1:10,000, Cat #7074P2, Cell Signaling Technology, Danvers, MA, USA) and goat anti-mouse IgG (1:10,000, Cat #7076P2, Cell Signaling Technology, Danvers, MA, USA) at room temperature for 1 h. Finally, the immunoblots were visualized using an enhanced luminescence kit (Cat #BL520A, Biosharp, Hefei, Anhui, China), and the intensity of the immunoblot bands was quantified using the ImageJ software. The original western blot figures are presented in the **Supplementary Material**.

2.10 Statistical Analysis

Experimental data are presented as mean $\pm$ standard deviation (SD) and median with minimum to maximum values. Statistical analyses were performed using GraphPad Prism 9.0 (GraphPad Software, San Diego, CA, USA). Quantitative data were analyzed using unpaired parametric tests, whereas rank data were analyzed using the nonparametric Wilcoxon's rank sum test. For data from multiple groups, a one-way analysis of variance (ANOVA) with Tukey's post-hoc test was used. Statistical significance was set at $p \leq 0.05$.

3. Results

3.1 Fingolimod Reduces Cerebral Infarction Volume, Alleviates Cerebral Edema, and Improves Neurological Function in MCAO/R Rats

TTC staining revealed no apparent damage to cerebral tissue in the sham group (Fig. 1A). On the contrary, rats in the MCAO/R group exhibited significant brain tissue lesions 1 d after cerebral ischemia or reperfusion injury (Fig. 1A). However, treatment with various fingolimod doses significantly reduced the volume of the cerebral infarct area in rats subjected to MCAO/R (Fig. 1A,B; $p < 0.001$). These results indicate that fingolimod treatment reduces the cerebral infarction volume on day 1 after cerebral ischemia or reperfusion.

To assess the effectiveness of fingolimod therapy in treating cerebral edema, the brain water content was determined one day post-reperfusion. The findings indicated that the rats subjected to MCAO/R had elevated water content in their cerebral tissues when compared to the rats in the sham group (Fig. 1C, $p < 0.001$). Nevertheless, the cerebral water content of MCAO/R rats treated with high-dose fingolimod (2.0 mg/kg) was markedly reduced when compared to MCAO/R group (Fig. 1C, $p < 0.001$). These findings indicate that a high dose of fingolimod alleviated cerebral edema induced by cerebral ischemia.

Additionally, to examine the effects of different dosages of fingolimod on the restoration of neurological function, we used the Zea-Longa Scale neurological score for each group. The results demonstrated that high-dose fingolimod administration (2.0 mg/kg) resulted in a statistically significant reduction in the neural function score compared to that in the MCAO/R group (Fig. 1D, $p < 0.05$). The findings suggest that treatment with fingolimod improves the neurological impairment induced by cerebral ischemia in rats after MCAO/R.

3.2 Fingolimod Inhibits Inflammation in Rats after MCAO/R

The levels of pro-inflammatory cytokines in serum, including TNF-α, IL-1β, and IL-6, were measured using ELISA to evaluate the potential anti-inflammatory efficacy of fingolimod in cerebral ischemia. The findings revealed that the serum levels of TNF-α, IL-1β, and IL-6 proteins were significantly higher in rats that underwent MCAO/R when compared to the levels observed in the sham-operated control group (Fig. 2A–C, $p < 0.001$). Nevertheless, the administration of fingolimod at multiple dosages resulted in a marked reduction in the serum IL-1β and IL-6 protein levels when compared to the MCAO/R group without treatment (Fig. 2A,B, $p < 0.01$, $p < 0.001$). Moreover, treatment with median and high doses of fingolimod led to an evident decrease in TNF-α levels compared to the MCAO/R group without treatment (Fig. 2C, $p < 0.001$). These findings imply that fingolimod protects against MCAO/R-caused brain injury by exerting its anti-inflammatory properties.

3.3 Fingolimod Downregulates HMGB1 Expression in MCAO Rats

The expression levels of HMGB1 following MCAO/R injury in rats were measured via western blot assays and immunohistochemical staining. Western blot analysis demonstrated an apparent increase in the levels of HMGB1 protein in the MCAO/R group when compared to the sham group (Fig. 3A,B; $p < 0.01$). In contrast, the expression levels of HMGB1 protein were considerably reduced in both the F-M and F-H groups as compared to the MCAO/R group (Fig. 3A,B; $p < 0.05$).

Additionally, we performed immunohistochemical analysis of HMGB1 in hippocampal slices from rats in

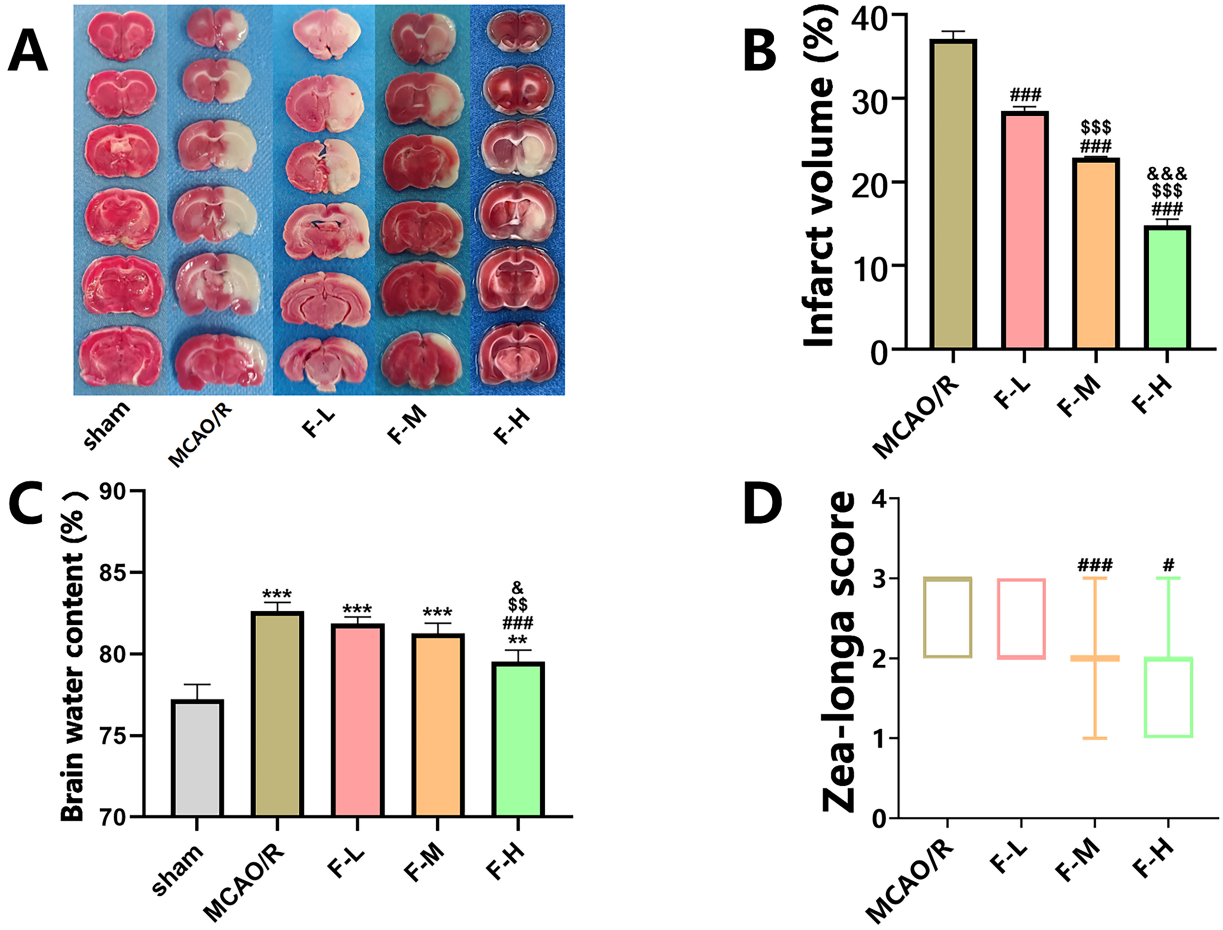

Fig. 1. Fingolimod effectively reduces cerebral infarction volume, alleviates cerebral edema, and improves neurological function in MCAO/R rats. (A) On the first day post-MCAO/R procedure, TTC staining images were captured, wherein the infarcted regions of the brain were depicted in white and the healthy regions in red. (B) Quantification of TTC staining (Data presented as mean ± SD, and analyzed using one-way ANOVA with Tukey's post-hoc test; N = 3). (C) Brain water content on day 1 after MCAO/R (Data presented as mean ± SD and analyzed using one-way ANOVA with Tukey's post-hoc test; N = 4). (D) The Zea-Longa score, indicative of neurological deficit, was evaluated one day post-MCAO/R, with data presented as the median along with the minimum and maximum values, and statistical analysis conducted using Wilcoxon's rank sum test (N = 15). $^{**}p < 0.01$ and $^{***}p < 0.001$ vs. sham group. $\#p < 0.05$ and $\#\#\#p < 0.001$ vs. MCAO/R group. $\$\$p < 0.01$ and $\$\$\$p < 0.001$ vs. F-L group. $\&p < 0.05$ and $\&\&\&p < 0.001$ vs. F-M group. MCAO/R, middle cerebral artery occlusion/reperfusion; TTC, 2,3,5-Triphenyltetrazolium Chloride; ANOVA, analysis of variance; F-L, fingolimod low-dose; F-M, fingolimod medium-dose; F-H, fingolimod high-dose; SD, standard deviation.

the different groups. Immunohistochemistry revealed HMGB1-positive protein deposition in both the cell nucleus and cytoplasm. The number of cytoplasm-positive HMGB1 staining cells was significantly higher in the MCAO/R group than in the sham group (Fig. 3C,D; $p < 0.001$). However, the quantity of cells exhibiting positive staining for HMGB1 in the cytoplasm was found to be reduced in both the F-M and F-H groups when compared to the MCAO/R group (Fig. 3C,D; $p < 0.05$, $p < 0.01$).

These results suggest that fingolimod treatment downregulated HMGB1 protein expression in MCAO/R rats. Additionally, fingolimod treatment inhibited the translocation of HMGB1 from the cell nucleus to cytoplasm to induced by cerebral ischemic injury.

3.4 Fingolimod Inhibits TLR4 Expression in MCAO Rats

The effect of various doses of fingolimod on TLR4 expression following MCAO/R injury in rats was evaluated using western blot assays and immunohistochemical staining.

Western blot analysis demonstrated that ischemic brain injury increased the expression level of TLR4 (Fig. 4A,B; $p < 0.05$). However, the medium and high doses of fingolimod treatment led to an apparent decrease in TLR4 levels (Fig. 4A,B; $p < 0.05$, and $p < 0.01$, respectively) compared to those in the MCAO/R group. These observations were supported by the immunohistochemical staining results. The count of TLR4-positive cells within the MCAO/R group was considerably greater than that ob-

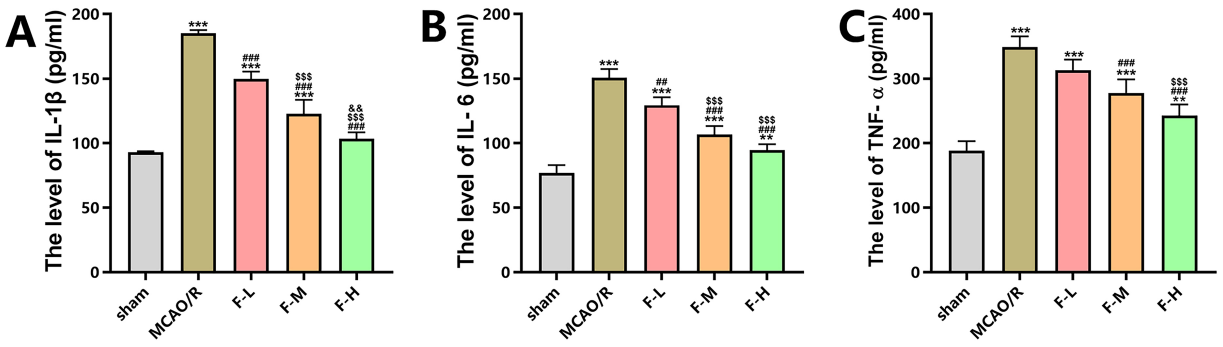

Fig. 2. Fingolimod inhibits inflammation in rats after MCAO/R. (A) Enzyme-Linked Immunosorbent Assay (ELISA) was employed to measure the serum concentrations of interleukin-1 beta (IL-1β) in rats, with data expressed as the mean ± SD and analyzed utilizing one-way ANOVA with Tukey's post-hoc test for multiple comparisons (N = 4). (B) Similarly, ELISA was utilized to ascertain the serum levels of interleukin-6 (IL-6) in rats, presenting data as mean ± SD and conducting analysis via one-way ANOVA with Tukey's post-hoc test (N = 4). (C) ELISA was also applied to quantify the serum levels of tumor necrosis factor alpha (TNF-α) in rats, with results depicted as mean ± standard deviation (SD), and statistical analysis performed using one-way ANOVA with Tukey's post-hoc test (N = 4). $^{**}p < 0.01$ and $^{***}p < 0.001$ vs. sham group. $\#\#p < 0.01$ and $\#\#\#p < 0.001$ vs. MCAO/R group. $\$\$\$p < 0.001$ vs. F-L group. $\&\&p < 0.01$ vs. F-M group.

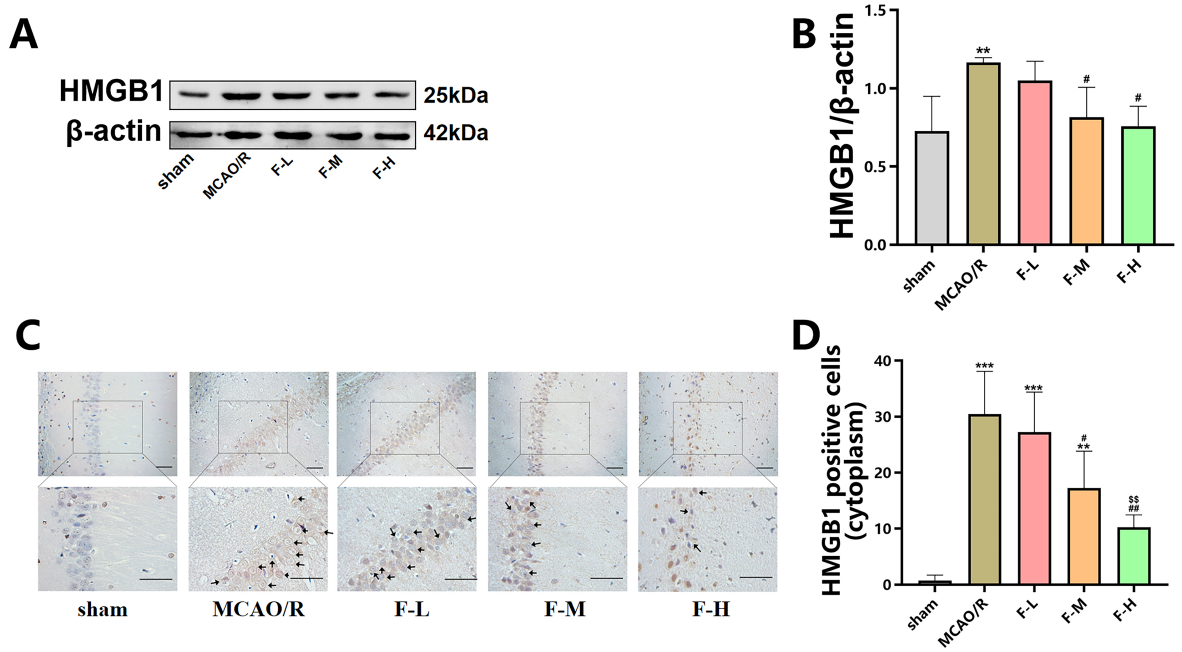

Fig. 3. Fingolimod down-regulates the expression of HMGB1 in MCAO/R rats. (A) The expression levels of HMGB1 within the hippocampal region of these rats were measured using the technique of western blot analysis, with the assessment being conducted day 1 post the MCAO/R procedure. (B) Quantification analysis of HMGB1 by western blot (Data presented as mean ± SD and analyzed using one-way ANOVA with Tukey's post-hoc test; N = 4). (C) Positive immunohistochemical staining for HMGB1. (D) Quantification of immunohistochemical staining for HMGB1 (Data presented as mean ± SD and analyzed using one-way ANOVA with Tukey's post-hoc test; N = 4). Scale bar = 50 µm. $^{**}p < 0.01$ and $^{***}p < 0.001$ vs. sham group. $\#p < 0.05$ and $\#\#p < 0.01$ vs. MCAO/R group. $\$\$p < 0.01$ vs. F-L group. HMGB1, high mobility group box 1.

served in the sham group (Fig. 4C,D; $p < 0.001$). On the contrary, a significant reduction in the number of TLR4-positive cells was noted in both the F-M and F-H groups when compared to the MCAO/R group (Fig. 4C,D, $p < 0.001$).

In summary, these results demonstrate that fingolimod treatment can effectively suppress the expression levels of TLR4 in rats that have undergone MCAO/R.

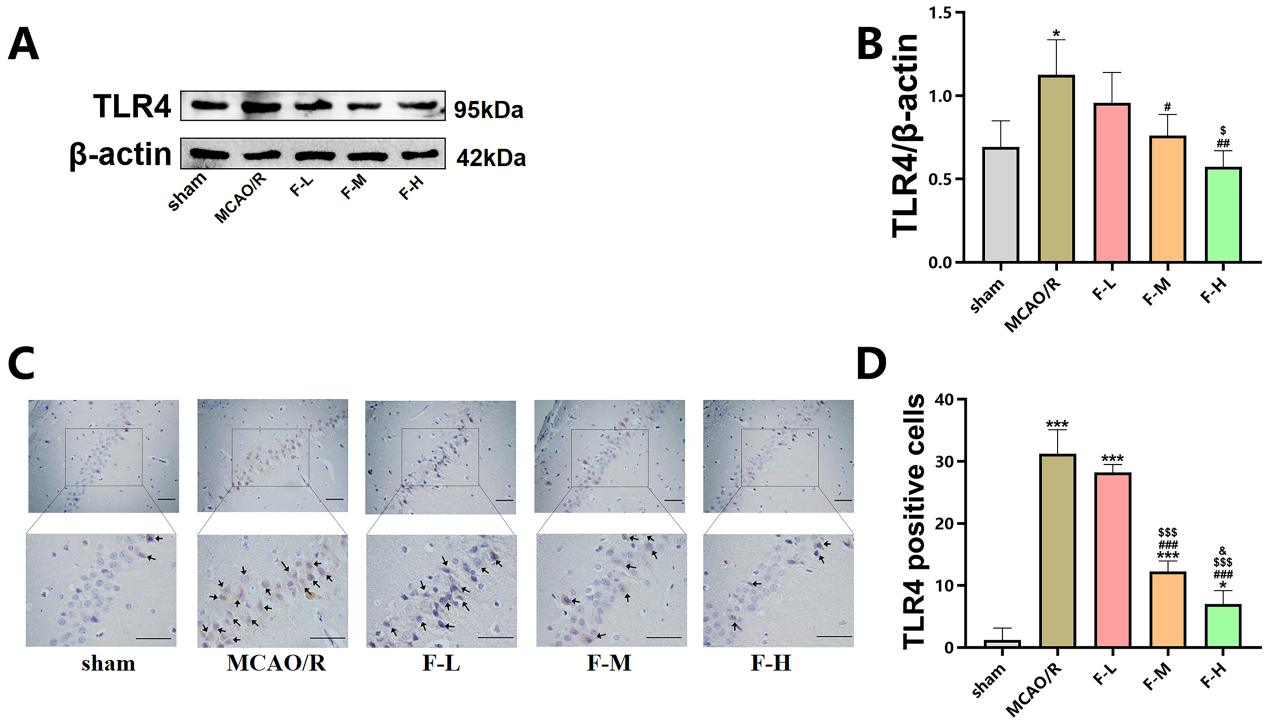

Fig. 4. Fingolimod inhibits TLR4 expression in MCAO/R rats. (A) The expression of TLR4 in the hippocampus of rats was detected using western blot analysis on day 1 after MCAO/R. (B) Quantification of TLR4 expression via western blot analysis (Data presented as mean ± SD and analyzed using one-way ANOVA with Tukey's post-hoc test; N = 4). (C) Immunohistochemical staining showing positive TLR4 expression. (D) Quantification of immunohistochemical staining for TLR4 (Data presented as mean ± S.D., and analyzed using one-way ANOVA with Tukey's post-hoc test; N = 4). Scale bar = 50 µm. *$p < 0.05$ and ***$p < 0.001$ vs. sham group. #$p < 0.05$, ##$p < 0.01$ and ###$p < 0.001$ vs. MCAO/R group. \$$p < 0.05$ and \$\$\$$p < 0.001$ vs. F-L group. &$p < 0.05$ vs. F-M group. TLR4, Toll-like receptor 4.

3.5 Fingolimod Treatment Decreases NF-κBp65 Level in MCAO Rats

To assess the impact of fingolimod treatment on NF-κBp65 protein expression following ischemic brain injury in rats, both western blotting and immunohistochemical staining techniques were utilized. The findings from the western blot analysis indicated a significant elevation in the levels of NF-κBp65 protein within the MCAO/R group when contrasted with the levels observed in the sham-surgery group (Fig. 5A,B; $p < 0.001$). Nevertheless, a notable reduction in the levels of NF-κBp65 protein was observed in both the F-M and F-H groups when compared to the levels found in the MCAO/R group. (Fig. 5A,B; $p < 0.01$, $p < 0.001$). These observations were supported by the immunohistochemical staining results. Immunohistochemistry revealed NF-κBp65-positive protein primarily deposition in the cell nucleus. The number of nuclear NF-κBp65-positive staining cells was significantly higher in the MCAO/R group than in the sham group (Fig. 5C,D; $p < 0.001$). Conversely, there were fewer nuclear NF-κBp65-positive staining cells in the F-M and F-H groups than in the MCAO/R group (Fig. 5C,D; $p < 0.05$, $p < 0.01$).

These findings provide compelling evidence that fingolimod treatment reduces the NF-κBp65 expression level in rats after ischemic brain injury. Additionally, treatment with fingolimod can inhibit the translocation of NF-κBp65 into the nucleus caused by cerebral ischemic/reperfusion injury.

4. Discussion

Ischemic stroke, which is primarily caused by ischemia or reperfusion brain injury, is a significant contributor to deaths globally [12]. Although early restoration of cerebral blood flow is crucial for reducing brain tissue injury, reperfusion can also cause secondary brain damage, including blood-brain barrier (BBB) damage and inflammation [13]. Consequently, mitigating the harmful impacts of cerebral ischemia and reperfusion has consistently been a central focus within extensive research efforts. Natural products have emerged as a significant source for drug development because of their minimal side effects and potent multi-target activity [14]. Fingolimod, a compound derived from *Cordyceps sinensis*, mitigates cerebral ischemic-reperfusion injury [15]. It easily traverses the BBB and accumulates in the brains of both humans and animals [16]. Additionally, fingolimod treatment enhances neurogenesis and facilitates repair in central nervous system injury models by activating endogenous neural precursor cells (NPCs)

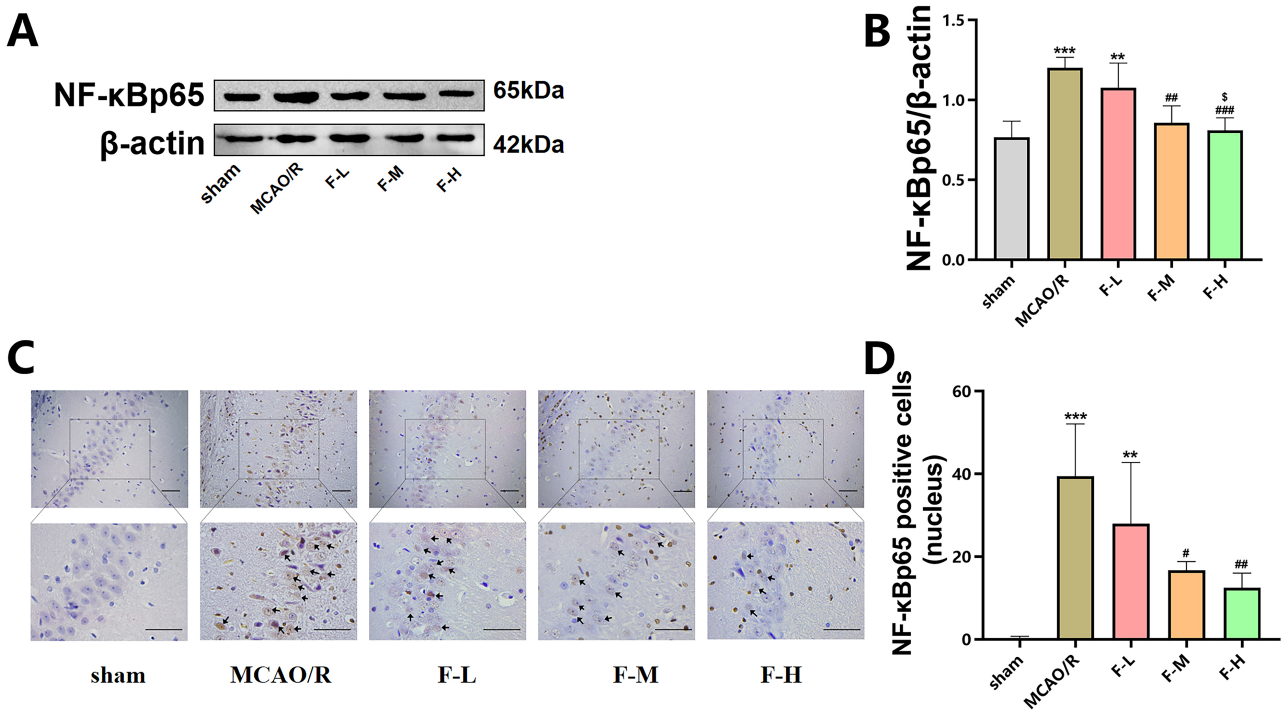

Fig. 5. Fingolimod treatment reduces NF-κBp65 expression in MCAO/R rats. (A) The expression of NF-κBp65 in the hippocampus of rats was detected using western blot analysis on day 1 after MCAO/R. (B) Quantification analysis of NF-κBp65 via western blot (Data presented as mean $\pm$ SD and analyzed using one-way ANOVA with Tukey's post-hoc test; N = 4). (C) Positive immunohistochemical staining for NF-κBp65. (D) Quantification of immunohistochemical staining for NF-κBp65 (Data presented as mean $\pm$ SD and analyzed using one-way ANOVA with Tukey's post-hoc test; N = 4). Scale bar = 50 µm. $^{**}p < 0.01$ and $^{***}p < 0.001$ vs. sham group. $\#p < 0.05$, $\#\#p < 0.01$ and $\#\#\#p < 0.001$ vs. MCAO/R group. $\$p < 0.05$ vs. F-L group. NF-κBp65, nuclear factor kappa-B p65.

or oligodendrocyte progenitors [17]. The objective of this research was to assess and compare the therapeutic efficacy of various doses of fingolimod in rats subjected to MCAO/R and explore the potential pharmacological mechanisms and molecular basis that underlie the drug's effects.

Our findings indicate that fingolimod treatment effectively mitigates brain edema, promotes recovery of neurobehavioral function, and provides neuroprotection following cerebral ischemia or reperfusion. Moreover, we observed a dose-dependent reduction in cerebral infarction volume following fingolimod treatment. Collectively, these results demonstrate that fingolimod possesses neuroprotective properties in a rat model characterized by transient focal cerebral ischemia.

Dysregulated inflammation significantly affects cerebrovascular diseases, particularly ischemic stroke [18]. Inflammatory mediators, including cytokines IL-1β, TNF-α, and IL-6, are elevated within a mouse model that simulates ischemic stroke, along with lymphocyte infiltration [19]. Interleukins are lymphokines involved in immune responses and have a significant impact on leukocyte and immune cell interactions [20]. IL-1β, for instance, promotes leukocyte migration to the lesion area, triggers inflammation, exacerbates blood-brain barrier dysfunction, and promotes apoptosis of damaged cells after ischemic stroke [21]. IL-6, produced by neurons, microglia, astrocytes, and endothelial cells in response to cerebral ischemic injury, is a poor prognostic factor for ischemic stroke [22]. TNF-α, which has a significant impact on the regulation of the inflammatory response, contributes to vasodilation, edema formation, adhesion of leukocytes and epithelium, oxidative stress, as well as inflammation [23]. A previous study reported that the levels of several inflammatory factors, including IL-1β, IL-6, and TNF-α, were elevated in rats with MCAO [24]. In our study, we observed that fingolimod administration reduced the levels of several inflammatory factors, including IL-1β, IL-6, and TNF-α, thereby suppressing excessive inflammatory responses caused by ischemia or reperfusion in brain injury.

Another important protein involved in early inflammatory responses is HMGB1. Research has shown that during cell injury, HMGB1, a highly conserved multifunctional protein, is moved from the nucleus to the cytoplasm and then actively secreted by immune cells like monocytes and macrophages, or released from necrotic cells [25,26]. It plays a crucial role in stimulating the production of TNF-α and IL-6, two key pro-inflammatory cytokines [26]. Interestingly, previous research has demonstrated a significant

increase in circulating HMGB1 levels in individuals with ischemic stroke within a few hours of symptom appearance [27]. Moreover, studies have confirmed that HMGB1, secreted into the extracellular environment by macrophages or monocytes, can activate astrocytes and microglia, leading to the release of other cytokines [28,29]. This process ultimately exacerbates ischemic brain injury in a rat model of cerebral ischemia. Downregulation of HMGB1, achieved using short hairpin RNA (shRNA), has been experimentally shown to suppress microglial activation, exert neuroprotective and anti-inflammatory effects, and reduce infarct volume in focal cerebral ischemia rat models [30]. Our study indicated that fingolimod treatment decreased HMGB1 protein levels in the hippocampus of rats with MCAO/R. Additionally, fingolimod treatment inhibited the translocation of HMGB1 from the cell nucleus to cytoplasm to induced by cerebral ischemic injury.

Toll-like receptor 4 (TLR4), a downstream receptor of HMGB1, has a significant effect on inflammatory responses [31]. HMGB1 triggers inflammatory signals by binding to its receptor for TLRs or advanced glycation end products, thereby activating a pro-inflammatory response [32]. A clinical trial has demonstrated that up-regulation of TLR4 expression is closely related to elevated serum levels of several inflammatory cytokines such as IL-1β, IL-6, TNF-α, and vascular cell adhesion molecule 1 (VCAM1) [33]. TLR4 expression is also independently correlated with lesion volume and poor prognosis in ischemic stroke patients [33]. Animal experiments have similarly shown that reducing the expression of TLR4 can decrease the brain infarct volume and improve neurological function in behavioral tests of mice subjected to MCAO [34,35]. AV411, also known as Ibudilast, is a TLR4 antagonist that exerts neuroprotective effects by inactivating microglia and inhibiting the secretion of inflammatory factors in animal models of acute cerebral ischemia [36,37]. Our findings are consistent with those of previous studies. Fingolimod treatment effectively reduced TLR4 expression in the hippocampus of rats with cerebral ischemia.

Nuclear factor kappa-B (NF-κB), a crucial downstream molecule of TLR4, is considered a vital transcription factor that participates in regulating various genes in the process of inflammatory response [38]. NF-κB is a heterodimer consisting of p50 and p65 subunits, and the nuclear translocation of NF-κBp65 from the cytosol to the nucleus indicates NF-κB pathway activation [39]. In its resting state, the NF-κB dimer binds to its inhibitor inhibitory kappa B (I-κB), existing in a deactivated form in the cytoplasm [40]. Upon receiving a stimulatory signal, such as lipopolysaccharide (LPS), the I-κB inhibitory protein undergoes phosphorylation at serine residues 32 and 36 by I-κB kinases (IKKs), leading to its ubiquitination and proteasomal degradation [41]. Activation of NF-κB promotes the secretion of several inflammatory cytokines TNF-α, IL-1β, IL-6, and interferon-γ, growth factors, immunoreceptors, and enzymes involved in oxidative stress, thereby exacerbating cerebral ischemia or reperfusion injury [42,43]. These findings suggest that suppressing the activation of NF-κB may be an effective therapeutic strategy against cerebral ischemia/reperfusion injury. In this research, we discovered that administering fingolimod resulted in a markedly decreased expression of the NF-κBp65 protein within the hippocampus of rats experiencing cerebral ischemia compared to the untreated group. Additionally, treatment with fingolimod can inhibit the translocation of NF-κBp65 into the nucleus caused by cerebral ischemic/reperfusion injury.

5. Conclusions

Our study provides evidence of the neuroprotective capabilities of fingolimod in ischemic stroke and sheds light on the underlying pharmacological mechanism of inflammation following ischemic stroke. We demonstrated that fingolimod treatment effectively reduced the volume of brain tissue infarction, alleviated brain edema, and promoted a dose-dependent recovery of neurological function in rats that underwent MCAO/R. Additionally, we observed that fingolimod exerted its anti-inflammatory effects by suppressing the HMGB1/TLR4/NF-κB pathway in the context of ischemia/reperfusion injury. Notably, a higher dose of fingolimod (2.0 mg/kg) yielded more favorable outcomes than the lower (0.5 mg/kg) and intermediate (1.0 mg/kg) doses in our study. These findings highlight the potential therapeutic value of fingolimod for the management of ischemic stroke-induced inflammation.

Availability of Data and Materials

The data will be available on reasonable request.

Author Contributions

LM, YL contributed to the conception and design of the study; YX, LZ, JG and CB contributed to the acquisition and analysis of data; YX and LZ contributed to drafting the text and preparing the figures. All authors contributed to editorial changes in the manuscript. All authors read and approved the final manuscript. All authors have participated sufficiently in the work and agreed to be accountable for all aspects of the work.

Ethics Approval and Consent to Participate

The animal procedures performed followed the guidelines of National Institutes of Health Guide for the Care and Use of Laboratory Animals and were approved by the Animal Care and Use Committee of Jinzhou Medical University (2022022701).

Acknowledgment

Not applicable.

Funding

This study was funded by the National Natural Science Foundation of China (Grant No. 81774116).

Conflict of Interest

The authors declare no conflict of interest.

Supplementary Material

Supplementary material associated with this article can be found, in the online version, at https://doi.org/10.31083/j.jin2308142.

References

[1] Zhang Z, He J, Wang B. Circular RNA circ_HECTD1 regulates cell injury after cerebral infarction by miR-27a-3p/FSTL1 axis. Cell Cycle. 2021; 20: 914–926.

[2] Grisotto C, Taïlé J, Planesse C, Diotel N, Gonthier MP, Meilhac O, *et al*. High-Fat Diet Aggravates Cerebral Infarct, Hemorrhagic Transformation and Neuroinflammation in a Mouse Stroke Model. International Journal of Molecular Sciences. 2021; 22: 4571.

[3] Xu J, Liu X, Luo L, Tang L, Guo N, Liu M, *et al*. A Metabonomics Investigation into the Therapeutic Effects of BuChang NaoXinTong Capsules on Reversing the Amino Acid-Protein Interaction Network of Cerebral Ischemia. Oxidative Medicine and Cellular Longevity. 2019; 2019: 7258624.

[4] Li S, Jiang D, Ehlerding EB, Rosenkrans ZT, Engle JW, Wang Y, *et al*. Intrathecal Administration of Nanoclusters for Protecting Neurons against Oxidative Stress in Cerebral Ischemia/Reperfusion Injury. ACS Nano. 2019; 13: 13382–13389.

[5] Wang JF, Mei ZG, Fu Y, Yang SB, Zhang SZ, Huang WF, *et al*. Puerarin protects rat brain against ischemia/reperfusion injury by suppressing autophagy *via* the AMPK-mTOR-ULK1 signaling pathway. Neural Regeneration Research. 2018; 13: 989–998.

[6] Wang Z, Kawabori M, Houkin K. FTY720 (Fingolimod) Ameliorates Brain Injury through Multiple Mechanisms and is a Strong Candidate for Stroke Treatment. Current Medicinal Chemistry. 2020; 27: 2979–2993.

[7] Porter H, Qi H, Prabhu N, Grambergs R, McRae J, Hopiavuori B, *et al*. Characterizing Sphingosine Kinases and Sphingosine 1-Phosphate Receptors in the Mammalian Eye and Retina. International Journal of Molecular Sciences. 2018; 19: 3885.

[8] Fu Y, Zhang N, Ren L, Yan Y, Sun N, Li YJ, *et al*. Impact of an immune modulator fingolimod on acute ischemic stroke. Proceedings of the National Academy of Sciences of the United States of America. 2014; 111: 18315–18320.

[9] Li F, Zhao H, Han Z, Wang R, Tao Z, Fan Z, *et al*. Xuesaitong May Protect Against Ischemic Stroke by Modulating Microglial Phenotypes and Inhibiting Neuronal Cell Apoptosis via the STAT3 Signaling Pathway. CNS & Neurological Disorders Drug Targets. 2019; 18: 115–123.

[10] Longa EZ, Weinstein PR, Carlson S, Cummins R. Reversible middle cerebral artery occlusion without craniectomy in rats. Stroke. 1989; 20: 84–91.

[11] Zou M, Al-Baradie RS, Al-Hindi H, Farid NR, Shi Y. S100A4 (Mts1) gene overexpression is associated with invasion and metastasis of papillary thyroid carcinoma. British Journal of Cancer. 2005; 93: 1277–1284.

[12] Xie W, Zhu T, Zhou P, Xu H, Meng X, Ding T, *et al*. Notoginseng Leaf Triterpenes Ameliorates OGD/R-Induced Neuronal Injury via SIRT1/2/3-Foxo3a-MnSOD/PGC-1α Signaling Pathways Mediated by the NAMPT-NAD Pathway. Oxidative Medicine and Cellular Longevity. 2020; 2020: 7308386.

[13] Asgari Taei A, Dargahi L, Khodabakhsh P, Kadivar M, Farahmandfar M. Hippocampal neuroprotection mediated by secretome of human mesenchymal stem cells against experimental stroke. CNS Neuroscience & Therapeutics. 2022; 28: 1425–1438.

[14] Qi F, Liu Y, Zhang K, Zhang Y, Xu K, Zhou M, *et al*. Artificial Intelligence Uncovers Natural MMP Inhibitor Crocin as a Potential Treatment of Thoracic Aortic Aneurysm and Dissection. Frontiers in Cardiovascular Medicine. 2022; 9: 871486.

[15] Zhu XY, Ma TT, Li Y, Zhang MQ, Zhao L, Liang J, *et al*. Fingolimod protects against neurovascular unit injury in a rat model of focal cerebral ischemia/reperfusion injury. Neural Regeneration Research. 2023; 18: 869–874.

[16] Newton J, Hait NC, Maceyka M, Colaco A, Maczis M, Wassif CA, *et al*. FTY720/fingolimod increases NPC1 and NPC2 expression and reduces cholesterol and sphingolipid accumulation in Niemann-Pick type C mutant fibroblasts. FASEB Journal. 2017; 31: 1719–1730.

[17] Blanc CA, Grist JJ, Rosen H, Sears-Kraxberger I, Steward O, Lane TE. Sphingosine-1-phosphate receptor antagonism enhances proliferation and migration of engrafted neural progenitor cells in a model of viral-induced demyelination. The American Journal of Pathology. 2015; 185: 2819–2832.

[18] Yang C, Wang X, Guo Y, Meng X, Li Y, Xia C, *et al*. Beneficial Effect of Edoxaban on Preventing Atrial Fibrillation and Coagulation by Reducing Inflammation *via* HBG1/HBD Biomarkers. Frontiers in Pharmacology. 2022; 13: 904317.

[19] Feng Y, Liao S, Wei C, Jia D, Wood K, Liu Q, *et al*. Infiltration and persistence of lymphocytes during late-stage cerebral ischemia in middle cerebral artery occlusion and photothrombotic stroke models. Journal of Neuroinflammation. 2017; 14: 248.

[20] Zhao X, Zhang Y, He W, Wei Y, Han S, Xia L, *et al*. Effects of Small Peptide Supplementation on Growth Performance, Intestinal Barrier of Laying Hens During the Brooding and Growing Periods. Frontiers in Immunology. 2022; 13: 925256.

[21] Zhu H, Hu S, Li Y, Sun Y, Xiong X, Hu X, *et al*. Interleukins and Ischemic Stroke. Frontiers in Immunology. 2022; 13: 828447.

[22] Yao H, Zhang Y, Shu H, Xie B, Tao Y, Yuan Y, *et al*. Hyperforin Promotes Post-stroke Neuroangiogenesis via Astrocytic IL-6-Mediated Negative Immune Regulation in the Ischemic Brain. Frontiers in Cellular Neuroscience. 2019; 13: 201.

[23] Bradley JR. TNF-mediated inflammatory disease. The Journal of Pathology. 2008; 214: 149–160.

[24] Bai Y, He Z, Duan W, Gu H, Wu K, Yuan W, *et al*. Sodium formononetin-3'-sulphonate alleviates cerebral ischemia-reperfusion injury in rats via suppressing endoplasmic reticulum stress-mediated apoptosis. BMC Neuroscience. 2022; 23: 74.

[25] García-Arnandis I, Guillén MI, Gomar F, Pelletier JP, Martel-Pelletier J, Alcaraz MJ. High mobility group box 1 potentiates the pro-inflammatory effects of interleukin-1β in osteoarthritic synoviocytes. Arthritis Research & Therapy. 2010; 12: R165.

[26] Kwak MS, Kim HS, Lee B, Kim YH, Son M, Shin JS. Immunological Significance of HMGB1 Post-Translational Modification and Redox Biology. Frontiers in Immunology. 2020; 11: 1189.

[27] Goldstein RS, Gallowitsch-Puerta M, Yang L, Rosas-Ballina M, Huston JM, Czura CJ, *et al*. Elevated high-mobility group box 1 levels in patients with cerebral and myocardial ischemia. Shock (Augusta, Ga.). 2006; 25: 571–574.

[28] Kim JB, Lim CM, Yu YM, Lee JK. Induction and subcellular localization of high-mobility group box-1 (HMGB1) in the postischemic rat brain. Journal of Neuroscience Research. 2008; 86: 1125–1131.

[29] Qiu J, Nishimura M, Wang Y, Sims JR, Qiu S, Savitz SI, *et al*. Early release of HMGB-1 from neurons after the onset of brain ischemia. Journal of Cerebral Blood Flow and Metabolism. 2008; 28: 927–938.

[30] Kim JB, Sig Choi J, Yu YM, Nam K, Piao CS, Kim SW, *et al*. HMGB1, a novel cytokine-like mediator linking acute neuronal death and delayed neuroinflammation in the postischemic brain. The Journal of Neuroscience. 2006; 26: 6413–6421.

[31] Singh GB, Zhang Y, Boini KM, Koka S. High Mobility Group Box 1 Mediates TMAO-Induced Endothelial Dysfunction. International Journal of Molecular Sciences. 2019; 20: 3570.

[32] Wang F, Lu Z, Hawkes M, Yang H, Kain KC, Liles WC. Fas (CD95) induces rapid, TLR4/IRAK4-dependent release of pro-inflammatory HMGB1 from macrophages. Journal of Inflammation. 2010; 7: 30.

[33] Brea D, Blanco M, Ramos-Cabrer P, Moldes O, Arias S, Pérez-Mato M, *et al*. Toll-like receptors 2 and 4 in ischemic stroke: outcome and therapeutic values. Journal of Cerebral Blood Flow and Metabolism. 2011; 31: 1424–1431.

[34] Caso JR, Pradillo JM, Hurtado O, Lorenzo P, Moro MA, Lizasoain I. Toll-like receptor 4 is involved in brain damage and inflammation after experimental stroke. Circulation. 2007; 115: 1599–1608.

[35] Cao CX, Yang QW, Lv FL, Cui J, Fu HB, Wang JZ. Reduced cerebral ischemia-reperfusion injury in Toll-like receptor 4 deficient mice. Biochemical and Biophysical Research Communications. 2007; 353: 509–514.

[36] Lee JY, Cho E, Ko YE, Kim I, Lee KJ, Kwon SU, *et al*. Ibudilast, a phosphodiesterase inhibitor with anti-inflammatory activity, protects against ischemic brain injury in rats. Brain Research. 2012; 1431: 97–106.

[37] Mizuno T, Kurotani T, Komatsu Y, Kawanokuchi J, Kato H, Mitsuma N, *et al*. Neuroprotective role of phosphodiesterase inhibitor ibudilast on neuronal cell death induced by activated microglia. Neuropharmacology. 2004; 46: 404–411.

[38] Zhu L, Carretero OA, Xu J, Harding P, Ramadurai N, Gu X, *et al*. Activation of angiotensin II type 2 receptor suppresses TNF-α-induced ICAM-1 via NF-κB: possible role of ACE2. American Journal of Physiology. Heart and Circulatory Physiology. 2015; 309: H827–34.

[39] Xu Y, Liu L. Curcumin alleviates macrophage activation and lung inflammation induced by influenza virus infection through inhibiting the NF-κB signaling pathway. Influenza and other Respiratory Viruses. 2017; 11: 457–463.

[40] Stancovski I, Baltimore D. NF-kappaB activation: the I kappaB kinase revealed? Cell. 1997; 91: 299–302.

[41] Lachman MF, Wright Y, Whiteman DA, Herson V, Greenstein RM. Brief clinical report: a 46,XY phenotypic female with Smith-Lemli-Opitz syndrome. Clinical Genetics. 1991; 39: 136–141.

[42] Kong L, Ma Y, Wang Z, Liu N, Ma G, Liu C, *et al*. Inhibition of hypoxia inducible factor 1 by YC-1 attenuates tissue plasminogen activator induced hemorrhagic transformation by suppressing HMGB1/TLR4/NF-κB mediated neutrophil infiltration in thromboembolic stroke rats. International Immunopharmacology. 2021; 94: 107507.

[43] Luo L, Liu M, Fan Y, Zhang J, Liu L, Li Y, *et al*. Intermittent theta-burst stimulation improves motor function by inhibiting neuronal pyroptosis and regulating microglial polarization via TLR4/NFκB/NLRP3 signaling pathway in cerebral ischemic mice. Journal of Neuroinflammation. 2022; 19: 141.